Polymer Nanostructures by Forced Assembly: Process, Structure, and Properties

Michael Ponting,[1] *Anne Hiltner,**[2] *Eric Baer*[2]

Summary: The process of micro- and nanolayer coextrusion of polymeric systems with good layer uniformity is described. Coextrusion through a series of layer multiplying die elements has enabled the production of films containing tens to thousands of layers with individual layer thicknesses from the micro- to the nanoscale. Improvements in layer uniformity are discussed through optimization of layer multiplier die design, selection of viscosity matched polymer systems, and incorporation of surface layer capabilities. Design of 'uneven' split layer multiplication dies has enabled the coextrusion of layered films with a wide variety of layer thickness distributions having up to a 10× difference in the individual film layer thicknesses. Coextrusion of layered polymer films with individual layer thicknesses down to the nanoscale has resulted in the production of novel systems with improved properties. Nanolayered polymer films were utilized to develop an all-plastic polymer laser, to fabricate gradient refractive index lenses, and to investigate gas barrier enhancement of crystalline polymer nanolayers confined to induce a high aspect ratio, in-plane, single-crystal-like lamellar structure.

Keywords: coextrusion; gas barrier; layer multiplication; nanolayers; photonics

Introduction

Polymeric structures and composites with properties superior to those of the individual components have been developed using various techniques including: polymer blending, block-copolymerization, and multilayer coextrusion. Layer-multiplying coextrusion represents an advanced polymer processing technique for combining two or more polymers in a layered configuration with controlled architecture. It is a continuous processing technique capable of economically producing films with up to thousands of layers with individual layer thicknesses from the micro- to the nanoscale.

Originally developed in the 1970s by the Dow Chemical Company,[1–5] early examples of synergistic polymer combinations in microlayered film systems included colorful iridescence,[6–8] crumple resistant gas and water barrier,[9] and increased ductility and impact strength which originate from changes in polymer deformation mechanisms as the layer thickness is reduced.[10–12] More recently, layered polymer films with micron-thick layers have seen increasing usage in composite films for packaging with improved gas barrier,[13] and increased mechanical toughness.[14,15] Commercialized technologies stemming from layered films with unique optical properties include highly reflective light filters[16,17] and polarizers.[18] As layer-multiplying coextrusion continues to evolve toward the nanoscale, opportunities arise to discover unique properties controlled by interfacial or confinement induced phenomena.

The advances in layer-multiplying technology and their application to novel

[1] Department of Chemical Engineering
[2] Department of Macromolecular Science and Engineering and Center for Layered Polymeric Systems, Case Western Reserve University Cleveland, OH 4410, USA
E-mail: pah6@case.edu

nanolayered polymeric material systems with improved properties are discussed in this article. The process is described with emphasis on recent improvements in layer uniformity and quality through optimized multiplying die design, polymer selection for matching rheology, and incorporation of polymeric surface layers. Based on these recent processing modifications, layered polymer systems with individual layer thicknesses ranging from microns down to tens of nanometers have been successfully coextruded.

Coextrusion of Micro- and Nanolayered Polymer Systems

Micro- and nanolayer coextrusion, the enabling technology of the National Science Foundation Center for Layered Polymeric Systems (CLiPS), utilizes a process of forced assembly through sequential layer multiplication to fabricate thin alternating layers of two or three polymers. The uniqueness of the coextrusion process lies in the combination of conventional coextrusion of two or more polymers in a layered feed-block with additional layer multiplication accomplished through a series of multiplier dies. This design creates a highly flexible, novel process for producing polymeric films with tens to thousands of layers. When the number of layers in a thin polymer film approach the thousands, individual layer thicknesses are reduced from the micron to the nanometer scale. This nanometer layer thickness can approach the radius of gyration of the individual polymer molecule. This highly ordered and constrained composite layered structures can enable the discovery of new phenomena which include the formation of totally interphase materials, a result of polymer chain interdiffusion on the scale of individual layer thicknesses, and confined crystallization, a procedure that induces frustrated crystallization and unique orientations in thin nanolayers due to spatial layer confinement. Through the production of these novel layered structures, discoveries relating to the physical and chemical properties of two or more nanolayered polymer compounds have been studied and utilized to develop systems with new and exciting properties.

Layer multiplication exploits the viscoelastic nature of polymer melts. A two component coextrusion system consisting of two $^{3}/_{4}$ inch single screw extruders with melt metering pumps, an (A/B) two layer coextrusion feedblock, a series of layer multiplying die elements, two laminating surface extruders, and an exit tape or film die is illustrated in Figure 1. The inclusion of metering pumps into the coextrusion

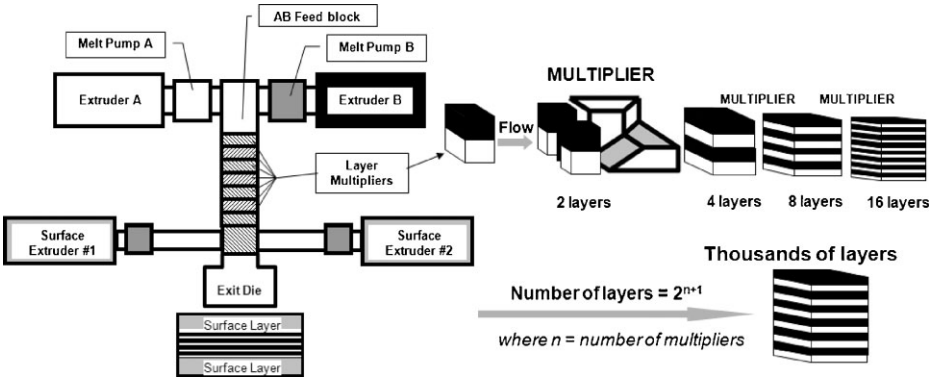

Figure 1.
(Left) Two component multilayer system comprised of extruders, pumps, feedblock, multiplying dies, surface layer extruders, and exit die. (Right) Schematic illustration of layer multiplication by cutting, spreading, and recombining the melt stream.

system enables an added degree of control over the relative thickness ratio of the layered polymers as they enter the A/B layered feedblock. From the feedblock, the two polymer layers enter a series of layer multiplication dies each of which doubles the number of layers through a process of cutting, spreading, and stacking the viscoelastic melt. A series of n multiplying elements combines two polymers as $2^{(n+1)}$ alternating layers as shown in Figure 1.

Figure 1 specifically illustrates how two-component coextrusion through a series of three multiplier elements increases the number of layers from 2 to 16. Coextruded polymers with up to eleven multiplier dies have produced films with 4096 layers and individual layer thicknesses below 10 nm.[19] Samples consisting of 2 to 4096 layers have been extruded in 1 to 2 mm tapes or film as thin 12 μm.

Added versatility in the coextrusion of dissimilar polymers with poor adhesion can be addressed by utilizing a three-component coextrusion system that incorporates an additional polymer as a tie layer (T) in an ATBTA sequenced feedblock. Combining the layer multiplication dies with a third tie-layer extruder allows for the introduction of thin adhesive or barrier layers into the multilayered polymer tapes and films as shown in Figure 2. Layer multiplication of three polymers in the ATBTA configuration through a series of n multipliers yields $2^{(n+2)}+1$ layers.

Improvements in layer uniformity and continuity have been addressed by matching polymer viscosities, by optimizing the layer multiplier die design, and by incorporating surface layers on the layered structure prior to film spreading. Layer uniformity and continuity strongly depend on the viscosities of the individual layered components. Poor viscosity matching can result in the lower viscosity polymer encapsulating the other by forming a slip film between the higher viscosity polymer and the multiplier die wall.[20] Interfacially driven layer instability and break-up may also result during layer multiplication if the two polymer melt streams possess a relatively large viscosity mismatch.[21] To maximize layer uniformity and overall film quality, polymers are extruded at a viscosity-match temperature and within a viscosity window determined by the coextrusion pressure (upper limit) and the melt strength (lower limit). Polymer viscosity is determined as a function of temperature using a Kayeness Galaxy 1 melt flow indexer at a low shear rate, 10 sec^{-1}. A low shear rate is selected to simulate polymer flow conditions in the layer multiplication dies. A typical plot of polymer viscosity against temperature, Figure 3, illustrates a good viscosity match

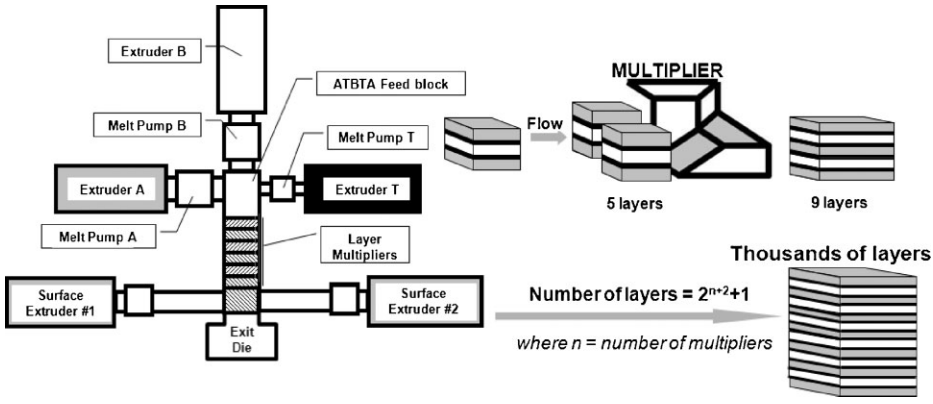

Figure 2.
(Left) Three component microlayer system with tie layer extruder. (Right) Schematic illustration of five to nine layer multiplication with a tie layer (T) separating the A and B layers.

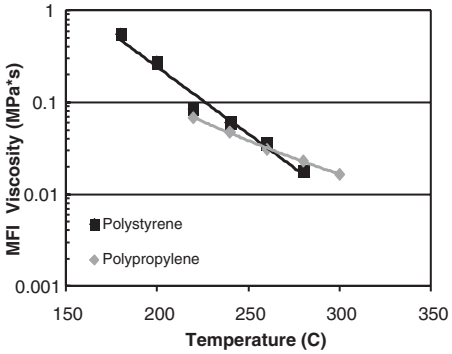

Figure 3.
The MFI viscosity match of PS/PP for determining microlayer coextrusion conditions.

at 260 °C for coextrusion of polypropylene (PP) and polystyrene (PS).

Design modifications to the multiplier elements were conducted to achieve a more uniform layer thickness distribution.[22] Based on model analysis, two multiplier designs were compared to investigate the effect of the layering pathlength, denoted as L and illustrated in Figure 4, on layer uniformity. Both designs utilized an identical approach of cutting, spreading, and stacking during layer multiplication. Design I, L = 15 cm, had a sharp spreading transition and short landings. Design II, L = 70 cm, possessed more gradual, rounded transitions and longer landings. The difference between the length spreading ratio BB′/AA′ and the stacking length ratio CC′/AA′ was reduced from 40% in Design I to 2% in Design II as a result of the longer die landing. The effect of multiplier design on layer uniformity was tested by coextrusion of a viscosity-matched polycarbonate (PC) and poly(methylmethacrylate) (PMMA) film. A 16 layer film with a 50/50 PC/PMMA composition was coextruded through a series of three Design I or Design II multiplier dies. To observe the individual layer uniformity from each multiplier design, cross-sections of the film were cut and polished with wet silicon carbide paper on a metallurgical wheel with individual layer thicknesses measured by polarized light microscopy, Figure 4.

The longer pathlength of the Design II multiplier dies resulted in much better layer uniformity, average layer thickness $69 \pm 8\,\mu m$, as compared to the Design I, average layer thickness $71 \pm 17\,\mu m$. Additionally, the smaller difference in the spreading and stacking path lengths of Design II dies eliminated the thick to thin tapering of layer thickness across the width of a single layer in films produced from Design I. Based on superior performance, Design II was utilized to obtain the structures discussed in this paper.

A breakthrough in the design of 'uneven' split layer multiplying dies enabled processing of films with a gradient in the layer thickness, Figure 5.[23] Coextrusion through a layer multiplying die with

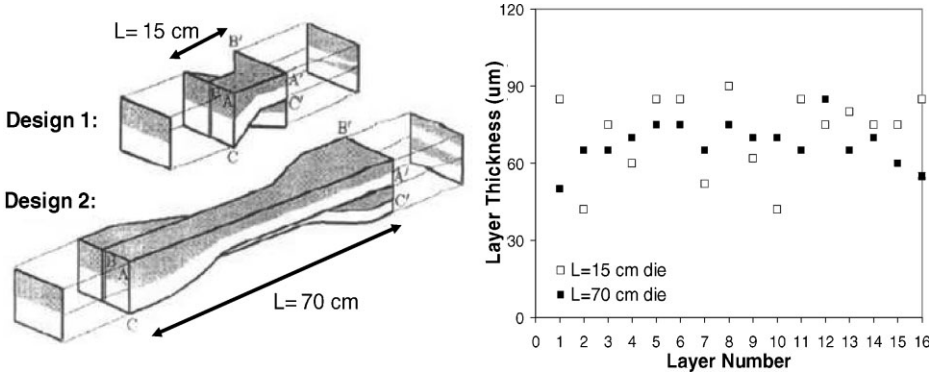

Figure 4.
(Left) Schematic illustrating the difference in polymer flow streamlines based on multiplier die length. (Right) The effect of increasing multiplier die length from 15 to 70 cm on layer uniformity.

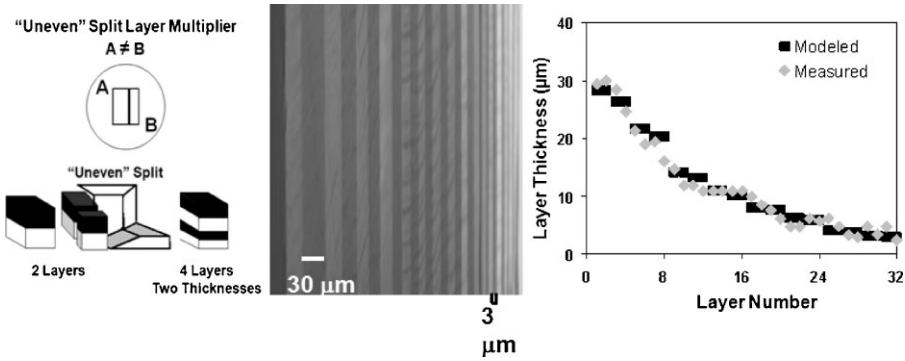

Figure 5.
(Left) Schematic illustrating 'uneven' split die multiplication producing two layer thicknesses. (Center) 32 layer PS/PMMA gradient film by coextrusion through four 'uneven' split dies to produce a 10× gradient in layer thickness. (Right) Comparison of the measured and the calculated layer thicknesses for a 32 layer PS/PMMA gradient film.

an uneven split in the feed channel width still resulted in the layer multiplication from two to four layers. However, when the melt stream was spread and recombined the two layers from the A side were thicker than the two layers from the B side, Figure 5. The ratio of the layer thicknesses emerging from the die was proportional to the A:B ratio. Four 'uneven' split layer multiplying dies were fabricated with varied feed channel ratios: 51:49, 52:48, 54:46, and 58:42. A 32 layer 10 mil film with a gradient in the layer thickness was produced by coextruding PS (Styron 615) and PMMA (VM-100) through these four 'uneven' split multipliers dies. The simulations predicted a 10× difference between the thickest and the thinnest layers. Individual layer thicknesses measured from film cross-section images exhibited an order of magnitude, 30 to 3 μm, difference in the thickest and the thinnest PS and PMMA layers.

Forced assembly coextrusion with 'uneven' split layer multipliers was not limited to producing large magnitude layer thickness gradients.

Combining the four previously described 'uneven' split layer multiplier dies with conventional 50:50 even split layer multipliers allowed for the coextrusion of films with larger number of layers and designed layer thickness distributions. The flexibility of the 'uneven' split layer multipliers was utilized to tailor the optical reflection band by varying the layer thickness distribution in 128 layer films. As an example, a 128 layer ''super lattice'' consisting of a blend of PMMA and poly(vinylidene fluoride) (PVDF) was coextruded with PS at a 60/40 feed ratio. This 128 layer film utilized four conventional multipliers with a 51:49 and a 52:48 'uneven' split multiplier, Figure 6.

The layer distribution obtained by combining an unbalanced 60/40 feed ratio with the 'uneven' split layer multipliers produced a dual reflection band within a single layered film, Figure 6. The optical effect of the ''super lattice'' distribution was the formation of two distinct reflection bands at 500 and 600 nm. The position, width, and intensity of these reflection peaks agreed well with theoretical modeling based on the layer thickness distribution and individual polymer refractive indices.[24] Dual reflection peak ''super lattice'' films have potential applications in the production of special optical filtering and sensory devices. The flexibility to rearrange and intermix the 'uneven' and the even split multipliers enables processing of a wide variety of layer thickness distributions that may lead to the production of novel polymeric structures for optical filters, information storage devices, and controlled release applications.

Further advances in film uniformity, in surface finish, and in overall flexibility in

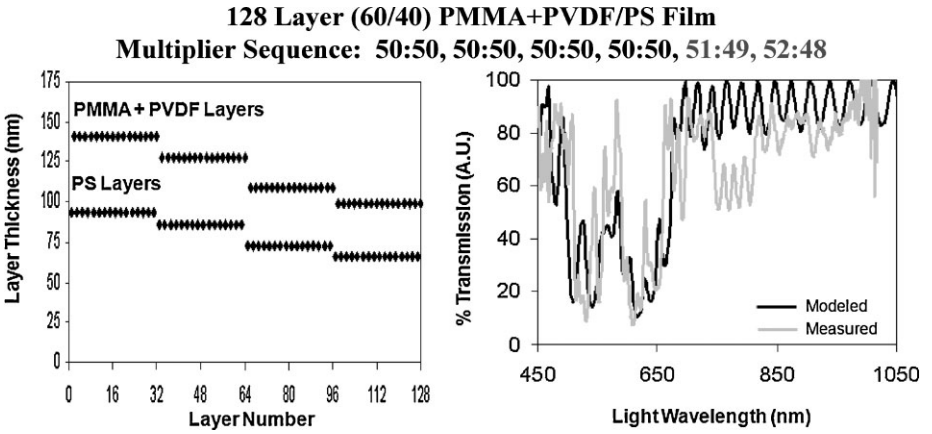

Figure 6.
(Left) Calculated "super lattice" thickness distribution for 128 layer film (Right) Comparison of modeled and measured reflection spectra.

the design of layered polymer structures is accomplished through the addition of post multiplication surface layers. A 3/4 inch single screw extruder and melt pump unit provide an upper and lower polymer layer on the layered polymer stream, Figures 1 and 2. This eliminates wall drag on the layered core during the final film spreading in the exit die. Sacrificial surface layers, i.e. top and bottom layers that can be peeled from the layered polymer core post-extrusion, significantly increase the layer uniformity and film surface quality.[25] Flexibility in the selection of an additional permanent surface layer provides another opportunity for improving mechanical, gas or water barrier, or optical properties of the layered system.

Recent processing advancements including a better understanding of polymer viscosity requirements for coextrusion, the optimization of layer multiplication die design, the development of 'uneven' split layer dies for gradient layer thickness films, and the addition of surface layers have enabled extension of layer-multiplying coextrusion to the nanoscale. In addition, successful coextrusion with as little as 50 grams of a specially synthesized material has demonstrated the nearly limitless design space available to fabricate polymer systems that possess novel optical, thermal, and gas barrier properties as a result of the hierarchical and scaling phenomena unique to individual polymer layers with nanoscale thicknesses.

Nanolayered Polymer Systems with Improved Properties

Coextrusion of layered polymer films with individual layer thicknesses down to the nanoscale have resulted in the production of novel systems with improved properties. Nanolayered polymer films were utilized to develop an all-plastic polymer laser, to fabricate gradient refractive index lenses, and to investigate gas barrier enhancement of crystalline polymer nanolayers confined to induce a high aspect ratio, in-plane, single-crystal-like lamellar structure.

1D Photonic Crystals and All-Plastic Lasers

Films with alternating layers of significantly different refractive indices and periodic nanolayer thicknesses approaching the quarter wavelength of light exhibit strong constructive optical reflections. Traditionally, reflective Bragg stacks have been produced by spin-coating inorganic materials with differing refractive indices.[26] Coextrusion of nanolayered polymers provides a method for continuous, low cost fabrication to extend highly reflective photonic technology to light weight

polymer materials. Optically reflective layered polymer films, referred to as 1D photonic crystals, were fabricated on the two component coextrusion system using the surface layer extruders and four multiplier die elements to produce 32 layer PS (Styron 615 APR) and PMMA (Plexiglas VM-100) films.[27] The PS ($n = 1.585$) and the PMMA ($n = 1.491$) were selected based on their difference in refractive index ($\Delta n = 0.09$) and compatible melt viscosities. To provide optimal PS/PMMA layer thickness uniformity, thick (13 μm) sacrificial low density polyethylene (LDPE 620I) surface layers were coextruded with the 2.8 μm thick photonic PS/PMMA layered core. An AFM cross-section image of a microtomed 32 layer PS/PMMA photonic film with well defined nanolayers, 86 nm ± 14 nm, is shown in Figure 7. The quality of the 32 layer 1D photonic crystal was evaluated by comparing the observed transmission spectrum with the simulated spectrum obtained by the matrix method of Vasicek[24] for a non-absorbing multilayer assembly of know refractive indices. A plot comparing the measured and simulated primary reflection band, Figure 7, displayed excellent agreement between not only the location of the primary reflection band, but also the intensity and the band width. A 1D photonic PS/PMMA film with a peak reflection slightly greater than 600 nm appeared as an orange to red colored film, however, flexibility in the coextrusion process allowed for altering the layer thickness to produce photonic films with other visible, ultra-violet, or near-infrared reflection bands.

The ability to design and rapidly fabricate many kilometers of highly reflective photonic crystal film enabled the development of advanced optical applications including potentially mass producible, all-plastic lasers. An all-plastic distributed Bragg reflector (DBR) laser was constructed by sandwiching a dye-doped active core layer between two highly reflective 128 layer PS/PMMA photonic crystal films with the reflection band designed to match the emission maximum of the dye.[28] Operation of the all plastic DBR laser was achieved through photo excitation ($\lambda_a = 532$ nm) of a Rhodamine 6G (R6G) laser dye (MW = 546 g/mole) doped in a PMMA monolith layer. The emitted light ($\lambda_e = 565$ nm) was reflected and redirected by the 1D photonic PS/PMMA film. Operation of the DBR all-plastic laser was successfully accomplished under a threshold of 90 μJ/cm^2 with a slope efficiently of 19.3%.

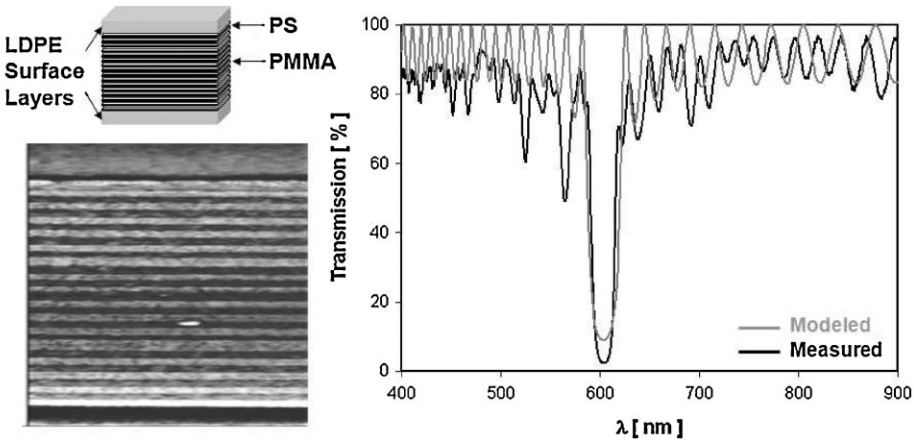

Figure 7.
(Left) Cross-section AFM of 32 layer PS/PMMA 1-D photonic film with LDPE surface layers. (Right) Comparison of measured and modeled transmission spectra of two stacked 32 layer PS/PMMA films with 86 nm average layer thickness.

A second all-plastic laser, a distributed feedback (DFB) design consisting of a single microlayered 1D photonic crystal film with active lasing dye chromophores in one layer, was successfully produced[29], Figure 8. In contrast to the DBR laser which required laminating 1D photonic crystal films to a dye-doped active layer, the DFB laser was produced in a single roll-to-roll microlayer processing step. Films with 128 alternating layers of a poly(styrene-co-acrylanitrile) with 25% wt. acrylonitrile content (SAN25) and a fluroelastomer terpolymer of vinylidene fluoride, hexafluoropropylene, and tetrafluorethylene (THV) (Dyneon 220G) were coextruded with sacrificial LDPE (DOW 620I) surface layers. The SAN25 ($n = 1.57$) and the THV ($n = 1.37$) were selected for coextrusion based on a substantial difference in refractive index ($\Delta n = 0.20$) and a good viscosity-match. The SAN25 was doped with 1.5 wt.% R6G dye. The THV had sufficiently low dye solubility to prevent diffusion of the R6G from the SAN25 layer. Coextrusion of SAN25 and THV layers 95 nm thick enabled the 1D photonic crystal reflection and the R6G fluorescence band to overlap and produced DFB lasing upon excitation with a Nd:YAG + OPO laser ($\lambda_e = 535$ nm). Lasing of the nanolayered SAN25/THV DFB laser occurred with efficiencies as high as 8% with excitation thresholds as low as 100 $\mu J/cm^2$. The high performance and potential low cost of continuous roll-to-roll microlayered DFB lasers demonstrated the technological usefulness of layer-multiplication already in practice in a range of passive devices.[18]

Nanolayer coextrusion of 1D photonic crystals is not limited to rigid glassy polymers. Highly elastic, tunable photonic crystals were produced through coextrusion of 128 layer films utilizing polyurethane (PU) ($n = 1.55$, Pellethane 2355-95AE) and Pebax ($n = 1.48$, Pebax 2533) elastomers.[27] Tunable 1D photonic crystals differ from the glassy PS/PMMA films in that very low stresses are necessary to induce reversible stretching or elongation of the elastomers. Elongation of the film decreases the overall film thickness and layer thickness, Figure 9, thereby changing the peak position of the reflection band. Transmission spectra of 128 layer PU/Pebax elastomeric photonic crystals were collected at increasing strain from 0 to 1.25. Stretching the elastomeric film to a strain of 1.25 resulted in a reversible reflection band shift from 600 nm (orange/red) to 400 nm (blue). The relationship between the applied strain, ε, and peak reflection, λ, is predictable based on geometric modeling of the film thinning during stretching. The reversibly tunable elastomeric 1D photonic crystals are another example of nanoscale layer thicknesses enabling a novel optical

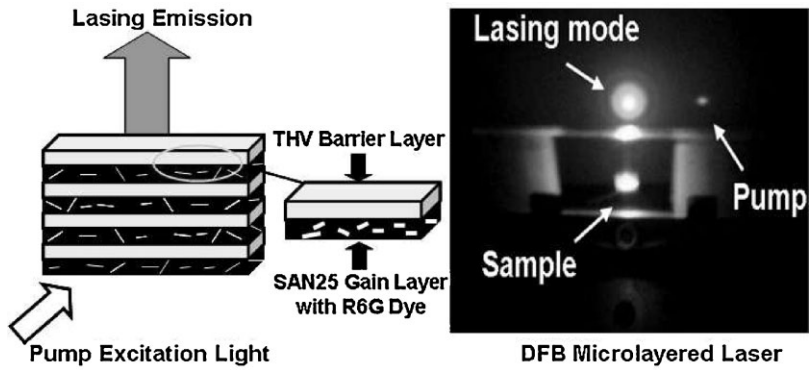

Figure 8.
(Left) Schematic of the DFB laser film of R6G doped SAN25 and THV. (Right) Lasing emission from the nanolayered DFB laser.

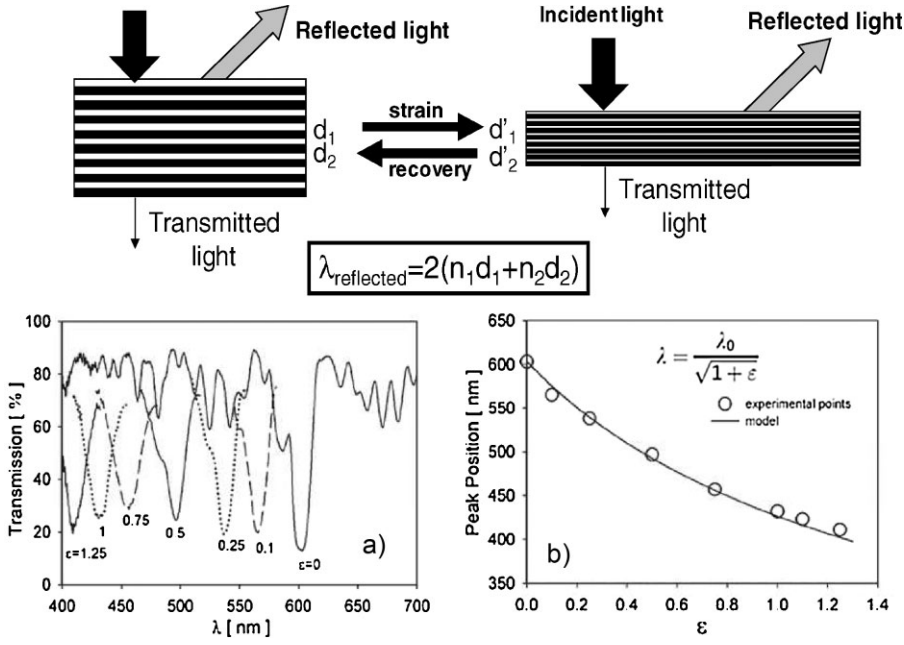

Figure 9.
(Left) Reflection spectrum as a function of wavelength at designated strains for an elastomeric 128 layer PU/Pebax tunable photonic crystal. (Right) Optical reflective peak position as a function of strain for tunable photonic crystal.

behavior in microlayered films that may lead to the development of new optically based strain sensor technology.

Variable Refractive Index Films for GRIN Lenses

Microlayer coextrusion provides additional flexibility by controlling the relative thicknesses of the A and B layers. Through coextrusion at off-set compositions, the relative thickness of PC and PMMA layers was varied from 1:1 at a 50/50 composition to 9:1 at a relative 90/10 composition, Figure 10.

The ability to vary the relative composition in a nanolayered polymer film with individual nanolayer thicknesses well below the quarter-wavelength of light allowed for creation of transparent layered films with designable refractive indices. A series of 4096 layer polymer films of PMMA (Plexiglas V920) and a styrene-acrylonitrile copolymer with 17% acrylonitrile content (SAN17) (Lustran) were coextruded at 1% composition intervals.[30] The refractive index of each of the 101 nanolayered PMMA/SAN17 films was measured and the results are plotted against overall film volume percentage of SAN17 in Figure 11.

Coextrusion of nanolayers less than the quarter-wavelength of light eliminates reflection as light passes from one layer to the next, which enables the nanolayers to act as a composite structure while remaining transparent to the visible eye. Varying the overall PMMA:SAN17 composition in the nanolayered film varies the composite film refractive index as a weighted average of the constituent polymers. Coextrusion of PMMA/SAN17 at 1% compositional intervals produced small, 0.0009 differences in the refractive index. Stacks of 101 films, each of different refractive index based on PMMA/SAN composition, were compressed under heat and pressure to produce a thick polymer sheet with a gradient in refractive index (GRIN) equal to the difference in refractive index of the nanolayered films. For variation of PMMA/SAN17 nanolayered films from 0/100 to

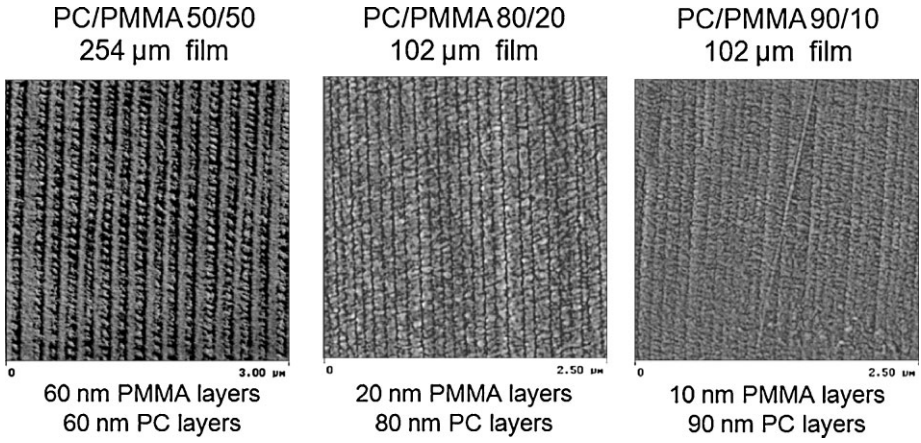

Figure 10.
Cross-section AFM image of PC (light) and PMMA (dark) layer films with (Left) 50/50 composition and 60 nm layers, (Center) Off-set 80/20 composition, and (Right) Off-set 90/10 composition.

100/0 compositions, a difference in refractive index of 0.09 was created. Subsequent shaping and polishing of this thick polymeric GRIN sheet produced polymeric GRIN lenses with a bio-inspired parabolic refractive index distribution. Improved optical image contrast and larger lens field of view resulted when GRIN lenses were compared with monolithic polymer or glass lenses of similar geometric shape.[30,31] Flexibility to create GRIN optics through stacking the variable refractive nanolayer films has enabled the design and production of nanolayered polymeric GRIN optics with unheralded freedom in the refractive index distribution. This breakthrough may enable lighter, higher powered optical information and imaging systems.

Nano-Confinement of Glassy and Crystalline Polymers

When two polymers are brought into contact, the interface is not perfectly sharp. The interphase between immiscible poly-

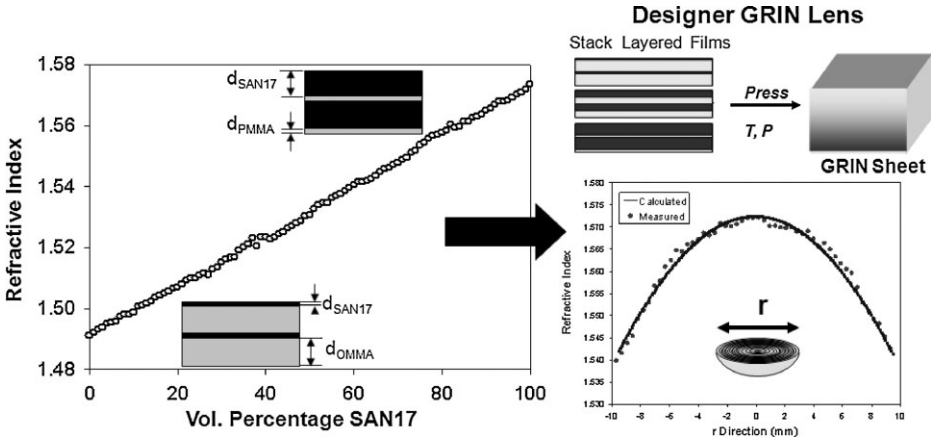

Figure 11.
Effect of composition on composite SAN17/PMMA film refractive index. Varying relative composition of SAN17/PMMA in the nanolayered film altered the refractive index of the composite nanolayered film leading to the production of novel gradient index lenses.

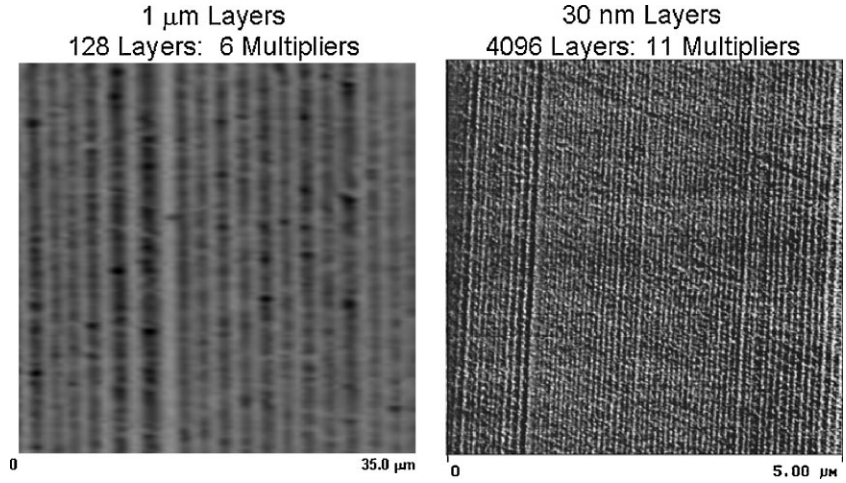

Figure 12.
(Left) Optical Micrograph of 128 layer 50/50 PC/PMMA film cross-section with 1 μm layers. (Right) AFM of 4096 layer 50/50 PC/PMMA film cross-section with 30 nm layers.

mer blends can be considered a third phased with its own characteristic properties.[32] Layer-multiplying coextrusion provides an opportunity to study the interphase through coextrusion of nanolayer films with individual polymer layer thicknesses approaching the 5 to 10 nm theoretical polymer interphase thickness.[33] Processing of 50/50 composition PC/PMMA multilayer films with layer thicknesses ranging the micro- to nanoscale was accomplished by increasing the total number of film layers from 128 up to 4096, Figure 12.

As individual layer thicknesses approach the interphase dimension, a new material is created that is totally interphase.[34] This totally interphase material was examined by utilizing DSC thermograms to track the T_g of PC and PMMA layers as a function of individual layer thickness, Figure 13.

When the individual layer thickness of the PC and PMMA was greater than 100 nm, T_gs near the constituent bulk values of 144 °C (PC) and 112 °C (PMMA) were measured. Decreasing layer thicknesses below 100 nm caused a gradual shift of the T_gs toward a single value. A single T_g was measured when the layer thicknesses were 10 nm or less, suggesting the transformation of the material from constituent layers to a totally interface material.[19] Layer-multiplying processing to produce polymer films with very thin layers provides for an opportunity to explore and create polymer materials with novel composite properties based on high interfacial interactions and confining nanolayer phenomena.[34–36]

Layer-multiplying coextrusion provides a flexible processing tool to decrease individual layer thicknesses through the microscale and approaching the nanoscale dimensions of

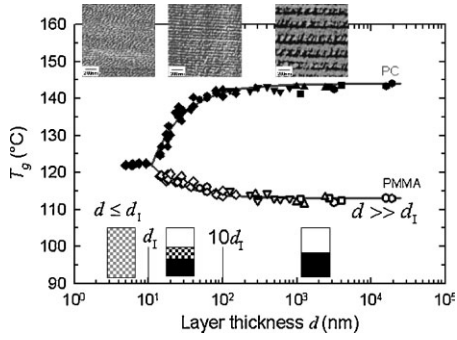

Figure 13.
The glass transition temperature of layered PC and PMMA layers as a function of individual layer thickness. As individual layer thickness is reduced into the nanoscale, increasing layer interphase contributions result in a convergence to an average T_g for PC and PMMA.

individual polymer molecules. Crystalline polymers confined in ultrathin spin-coated layers,[37,38] or microphase separated block structures containing at least one crystallizable block,[39] have produced specific crystal orientations and unique lamellar morphologies. One dimensional confinement of crystalline polymers by layer-multiplying coextrusion provides an advantage over the preceding techniques in the ability to achieve long range, defect free nano-confinement in films with thousands of individual layers. As a result of the structural plurality of the confined crystalline layers in a composite film, the use of conventional polymer analysis techniques can be utilized to probe structure-property relationships.

A series of layered polymer films of alternating polyethylene oxide (PEO) (Polyox) and either PS (Styron 615) or poly(ethylene-co-acrylic acid) (EAA) (Primacor) were coextruded.[40,41] The layer thickness of PEO was systemically decreased from 10 μm to 10 nm, the reported thickness of PEO crystalline lamellae, by tuning the relative composition of PEO/PS or PEO/EAA and increasing the overall number of film layers from 9 to 1025. Cross-section AFM images of microtomed PEO/PS layers with individual PEO layer thickness ranging from 1 μm to 25 nm were examined to elucidate structural implications of confinement on the PEO layer crystalline structure, Figure 14.

Truncated spherulites, resembling the bulk PEO crystallization habit, were prevalent in thicker, microscale PEO layers. In the 300 nm layers, confinement by PS appeared to highly constrain the growth direction of the PEO lamellae resulting in a preferential orientation in the layer plane. Further reduction of layer thickness to 75 nm resulted in PEO layers crystallizing as in-plane stacks of three to five long lamellae. Finally, in 25 nm layers, the PEO was confined to crystallize into very long, in-plane, single crystal-like lamellae sandwiched between thick PS layers. To confirm the observed increased PEO lamellar orientation when confined in very thin nanolayers, wide angle X-ray scattering (WAXS) patterns were measured in the extrusion direction (ED), Figure 14. In good agreement with the AFM images, PEO (120) WAXS reflection patterns exhibited increasing equatorial orientation from the two arc pattern in 1 μm PEO layers to highly oriented fiber-like spot patterns in 25 nm layers. The sharpness of the diffraction spots in the 25 nm PEO layer WAXS pattern suggested that PEO crystals were well oriented in-plane in the PEO confined layer.

The effect of in-plane orientation of large PEO single crystal layers on the oxygen permeability of PEO/EAA and PEO/PS nanolayer films was tested in a Mocon OxTran® permeability unit at 23 °C

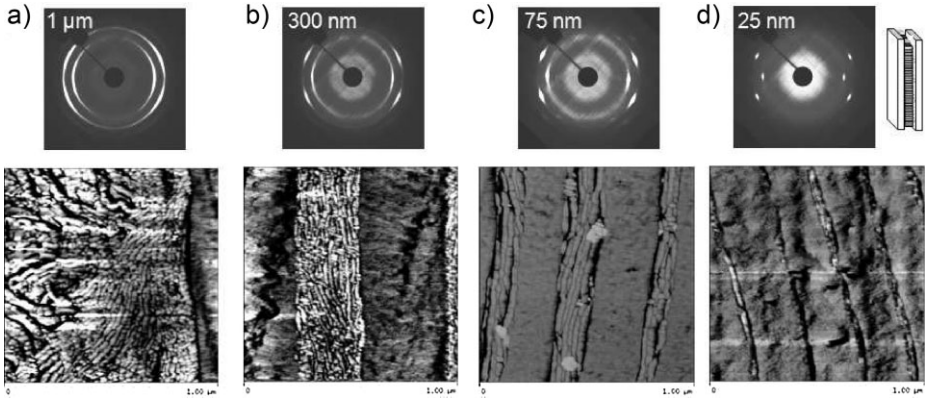

Figure 14.
2D WAXS extrusion direction patterns and AFM cross-section images exhibiting lamellar orientation in PS/PEO layered films with nominal PEO layer thickness of (a) 1 μm, (b) 300 nm, (c) 75 nm, and (d) 25 nm.

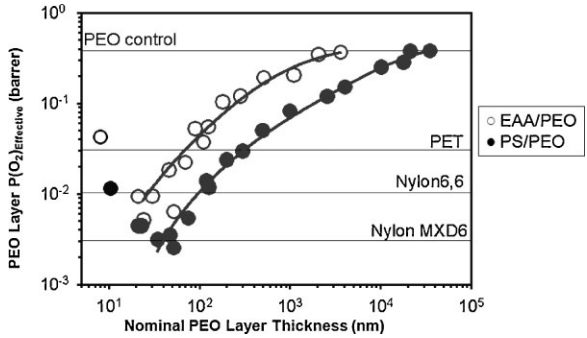

Figure 15.
Oxygen permeability of polyethylene oxide (PEO) layer as a function of PEO layer thickness in PEO/PS and PEO/EAA micro- and nanolayer films. Oxygen permeability tests were conducted at 23 °C and 0% relative humidity.

and dry conditions. Effective PEO layer oxygen permeability as a function of layer thickness was calculated from the measured oxygen flux using the series transport model for layered structures, Figure 15.[41]

As PEO layer thickness was reduced below a micron, a smooth decrease in effective PEO oxygen permeability with decreasing layer thickness was measured. A minimum effective PEO layer oxygen permeability of 0.0025 barrer was measured for confined, highly oriented 25 nm PEO layers. This was nearly 150 times lower than the bulk PEO permeability, 0.38 barrer. The large improvement in confined PEO layer oxygen barrier was attributed to the large size, estimated to approach 5 microns, of the gas impermeable, single crystal-like, in-plane lamellae induced through nanolayer confinement.

Conclusion

Layer-multiplying coextrusion was demonstrated as a polymer processing technology capable of producing films with up to thousands of layers with layer thicknesses in the micro- and nanoscale. Production of nanolayer films was demonstrated with improved layer uniformity stemming from optimization of layer multiplier die design, selection of viscosity matched materials, and incorporation of surface layer capabilities. Design of 'uneven' split layer multiplier dies enabled the coextrusion of a wide variety of layer thickness distributions. Layered films with improved properties were successfully coextruded based on nanoscale structure-property relationships. Optical properties of nanolayer polymer films were utilized to produce an all-polymer laser, tunable photonic materials for sensors, ''super lattice'' dual reflection peak films, and novel GRIN lenses. Coextrusion of a semi-crystalline polymer in 25 nm thick layers led to gas barrier enhancement based on a layer confinement induced crystalline phase orientation. The ability of layer-multiplying coextrusion to produce synergistic composite structures by a continuous process with only minimal material quantities continues to make it an attractive tool for rapid development of a broad range of future polymeric materials and composites based on novel structure-property relationships.

Acknowledgements: This research was supported by the *NSF Center for Layered Polymeric Systems* (grant DMR-0423914).

[1] U.S. Patent 3,565,985, **1971**.
[2] U.S. Patent 3,711,176, **1973**.
[3] U.S. Patent 3,884,606, **1975**.
[4] U.S. Patent 5,094,788, **1990**.
[5] U.S. Patent 5,269,995, **1993**.
[6] U.S. Patent 3,576,707, **1971**.
[7] U.S. Patent 5,389,324, **1995**.
[8] A. J. Radford, T. Alfrey Jr., W. J. Schrenk, *Polym. Eng. Sci.*, **1973**, *13*, 216.
[9] W. J. Schrenk, T. Alfrey Jr., *Polym. Eng. Sci.*, **1969**, *9*, 393.

[10] B. Gregory, A. Hiltner, E. Baer, J. Im, *Polym. Eng. Sci.*, **1987**, *27*, 568.
[11] B. Gregory, A. Siegmann, J. Im, A. Hiltner, E. Baer, *J. Mat. Sci.*, **1987**, *22*, 532.
[12] J. Im, E. Baer, A. Hiltner, in: "*High Performance Polymers*", E. Baer, A. Moet, Eds., Hanser Publishers, New York **1991**, p. 175.
[13] M. Gupta, Y. Lin, T. Deans, A. Crosby, E. Baer, A. Hiltner, D. Schiraldi, *Polymer*, **2009**, *50*, 598.
[14] C. D. Mueller, S. Nazarenko, T. Eberling, T. Schuman, A. Hiltner, E. Baer, *Polym. Eng. Sci.*, **1997**, *37*, 355.
[15] J. Kerns, A. Hsieh, A. Hiltner, E. Baer, *J. Appl. Polym. Sci.*, **2000**, *77*, 1545.
[16] U.S. Patent 6,830,713, **2001**.
[17] S. G. Johnson, J. D. Joannopolous, "*Photonic Crystals-The Road from Theory to Practice*", 1st ed., Kluwer Academic Publishers, Boston **2000**.
[18] M. F. Weber, C. A. Stover, L. R. Gilbert, T. J. Nevitt, A. J. Ouderkirk, *Science*, **2000**, *287*, 2451.
[19] R. Y. F. Liu, Y. Jin, A. Hiltner, E. Baer, *Macromol. Rapid Commun.*, **2003**, *24*, 943.
[20] W. Michaeli, "*Extrusion Dies for Plastics and Rubber: Design and Engineering Computations*", Hanser Publishers, New York **1992**.
[21] W. J. Schrenk, T. Alfrey Jr., "Coextruded Multilayer Polymer Films and Sheets" in: *Polymer Blends*, Vol. 2, D. R. Paul, S. Newman, Eds., Academic Press **1978**, p. 129.
[22] E. Baer, J. Kerns, A. Hiltner, in: "*Structure Development During Polymer Processing*", A. M. Cunha, S. Fakirov, Eds., Kluwer Academic Publishers, Netherlands **2000**, p. 327.
[23] M. Ponting, A. Hiltner, E. Baer, "*Gradient Multilayered Films by Forced Assembly Coextrusion*" *ANTEC 2009 – Proceedings of the 67th Annual Technical Conference & Exhibition*, **2009**, 67, 796.
[24] A. Vasicek, "*Optics of Thin Films*", 1st ed., North-Holland Publishing Co, Netherlands **1960**.
[25] T. E. Bernal-Lara, A. Ranade, A. Hiltner, E. Baer, in: "*Mechanical Properties of Polymers Based on Nanostructure*", 1st ed., G. H. Micheler, F. Balta-Callaja, Eds., CRC Press, Boca Raton, Florida **2005**, 629.
[26] T. Komikado, A. Inoune, K. Masuda, T. Ando, S. Umegaki, *Thin Solid Films*, **2007**, 3887.
[27] T. Kazmierczak, H. Song, A. Hiltner, E. Baer, *Macromol. Rapid Commn.*, **2007**, *28*, 2210.
[28] K. D. Singer, T. Kazmierczak, J. Lott, H. Song, Y. Wu, J. Andrews, E. Baer, A. Hiltner, C. Weder, *Optics Express*, **2008**, *16*, 10358.
[29] H. Song, K. D. Singer, J. Lott, Y. Wu, J. Zhou, J. Andrews, E. Baer, A. Hiltner, C. Weder, *Chem. Matr.*, accepted **2008**.
[30] Y. Jin, H. Tai, A. Hiltner, E. Baer, J. S. Shirk, *J. Appl. Polym. Sci.*, **2007**, *103*, 1844.
[31] G. Beadie, J. S. Shirk, A. Rosenberg, P. A. Lane, E. Fleet, A. R. Kamdar, Y. Jin, M. Ponting, Y. Yang, T. Kazmierczak, A. Hiltner, E. Baer, *Optics Express*, **2008**, *16*, 11540.
[32] L. A. Utracki, in: "*Polymer Alloys and Blends: Thermodynamics and Rheology*", Hanser Publishers, Munich **1990**, p. 118.
[33] G. D. Merfeld, D. R. Paul, in: "*Polymer Blends*, Vol. 1", D. R. Paul, C. B. Bucknall, Eds., Wiley, New York **2000**, p. 55.
[34] R. Y. F. Liu, A. P. Randae, H. P. Wang, T. E. Bernal-Lara, A. Hiltner, E. Baer, *Macromolecules*, **2005**, *38*, 10721.
[35] R. Y. F. Liu, T. E. Bernal-Lara, A. Hiltner, E. Baer, *Macromolecules*, **2005**, *38*, 4819.
[36] R. Y. F. Liu, T. E. Barnal-Lara, A. Hiltner, E. Baer, *Macromolelcules*, **2004**, *37*, 6972.
[37] C. W. Frank, V. Rao, M. M. Despotopoulou, R. F. W. Pease, W. D. Hinsberg, D. R. Miller, J. F. Rabolt, *Science*, **1996**, *273*, 912.
[38] G. Reiter, I. Botiz, L. Graveleau, N. Grozev, K. Albrecht, A. Mourran, M. Moeller, *Lecture Notes in Physics*, **2007**, *714*, 179.
[39] L. Zhu, S. Z. D. Cheng, B. H. Calhoun, Q. Ge, R. P. Quirk, E. L. Thomas, B. S. Hsiao, F. Yeh, B. Lotz, *J. Am. Chem. Soc.*, **2000**, *122*, 5957.
[40] H. Wang, J. K. Keum, A. Hiltner, E. Baer, B. D. Freeman, A. Rozanski, A. Galeski, *Science*, **2009**, *323*, 757.
[41] H. Wang, J. K. Keum, B. D. Freeman, A. Hiltner, E. Baer, *Macromol. Rapid Commn.*, submitted **2009**.

